THE STABILITY ANALYSIS OF DYNAMIC SPECT SYSTEMS

J.M. BORWEIN * AND W. SUN †

Abstract. SPECT (Single Photon Emission Computed Tomography) techniques have been applied to a wide range of medical studies. The stability of a SPECT model depends strongly upon the data collected. We show that a SPECT model is full rank and well-conditioned (stable) if the projection data are large enough. Condition number estimates for a linear model are given. Numerical results for a class of linear models confirm our theoretical analysis.

Key words. SPECT model, least squares, stability, medical imaging.

AMS subject classifications. 68U10, 41A30, 65F35

1. Introduction. SPECT (**Single Photon Emission Computed Tomography** is one of the more popular techniques in image processing. In many medical imaging studies, the distribution of some physical property of interest in the object (phantom, animal or patient) is time-dependent [1,7,10]. For example, the distribution function in fatty acid myocardial viability studies is assumed to be [5]

$$g(x,y,t) \equiv A(x,y)e^{-\lambda(x,y)t} + B(x,y)e^{-\eta(x,y)t} + C(x,y) \tag{1.1}$$

in a two-dimensional image. To reconstruct this image $A(x,y)$, $B(x,y)$, $C(x,y)$, $\lambda(x,y)$ and $\eta(x,y)$ must be estimated from the projections of activity distribution. The projection data are estimates of line integrals of this function. As shown in Figure 1, each line can be specified by two variables s and t. Since the detector is moving around the object being observed and the different projections corresponding to different angles are acquired at successive time intervals, for simplicity t represents both time and angle. Then

$$\int_{\Gamma(s,t)} g(s,z,t)dz = d(s,t), \qquad (s,t) \in \Omega \equiv [0,\sqrt{2}] \times [0,T]. \tag{1.2}$$

A great deal of effort has been dedicated to efficient solution of the above integral equation in the past eighty years [2,8,9]. In this paper, we are concerned with a least squares method. For simplicity, we assume that the reconstructed image is a unit square, $[0,1] \times [0,1] \subset R^2$ and $\{x_{i_1}, y_{i_2}\}_{i_1,i_2=1}^{I_1}$ denotes a uniform partition in this image which is divided into $I = I_1^2$ pieces (pixels). At each pixel, the distribution function is assumed to be a constant, *i.e.*,

$$g(x,y,t) = A_i e^{-\lambda_i t} + B_i e^{-\eta_i t} + C_i \equiv \xi_i(t), \qquad \text{in the i-th pixel.} \tag{1.3}$$

Then the integral equation (1.2) can be rewritten as

$$\sum_{i=1}^{I} a_{ijk}\xi_i(t_k) = d_{jk}, \quad j = 1,2,...,J \text{ and } k = 1,2,...,K, \tag{1.4}$$

* Centre for Experimental and Constructive Mathematics (CECM), Simon Fraser University, Burnaby, BC V5A 1S6, Canada (jborwein@cecm.sfu.ca). The work of this author is supported in part by the Natural Science and Engineering Research Council of Canada (NSERC).

† Centre for Mathematics & its Applications, School of Mathematical Sciences, Australian National University, Canberra, ACT 0200 Australia (weiwei@maths.anu.edu.au). The work of this author is supported in part by the Natural Science and Engineering Research Council of Canada (NSERC) Research grants of Dr J. Borwein and Dr R.D. Russell.

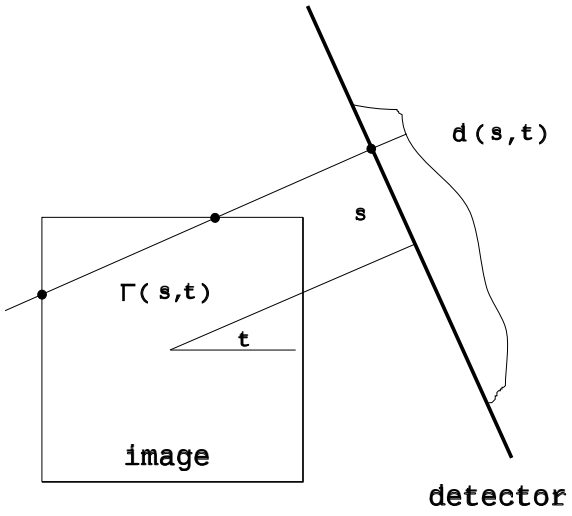

FIG. 1. *Projection-measurement geometry.*

where J and K represent the numbers of bins and projections, respectively, $d_{jk} = d(s_j, t_k)$ and a_{ijk} represents the length of the intersection of the jth ray (bin) coming from the angle of the kth projection within the ith pixel. Then this dynamic SPECT model can be formulated as the following least squares problem:

$$\min r(\boldsymbol{b}, \boldsymbol{\beta}) \equiv \sum_{j,k} \left(d_{jk} - \sum_i a_{ijk} \xi_i(t_k) \right)^2 . \tag{1.5}$$

where

$$\begin{aligned} \boldsymbol{b} = (b_i) &\equiv (A_1, B_1, C_1, ..., A_I, B_I, C_I)^T \in \mathbb{R}^{3I} \\ \boldsymbol{\beta} = (\beta_i) &\equiv (\lambda_1, \eta_1, ..., \lambda_I, \eta_I)^T \in \mathbb{R}^{2I}. \end{aligned} \tag{1.6}$$

Least squares approach for SPECT model was considered by many authers (*e.g.*, see [3,6]).

A serious problem in practice is how to choose the J and K. Obtaining suitable J and K are of significant importance for the stability of model, the accuracy of data measurement and the convenience of patients. However, due to the lack of theoretical analysis this has not been paid much attention. Dynamic SPECT models arising in medical study are often unstable. The least squares solution for such an unstable model is correspondingly inaccurate. Noise in the practical data measurement is unavoidable and makes the problem more serious. In this paper, we shall study the stability of this dynamic SPECT model.

The organization of this paper is as follows. In Section two, we give a matrix decomposition formulation which is a tool for our analysis. In Section three, we discuss the stability of a class of SPECT models and show that the models are full rank and well-conditioned if the projection data are large enough. An estimate of the condition number is given. Finally, we present some numerical experiments in Section four, which confirm our theoretical analysis.

2. A Class of Least Square Problems. This underlying SPECT problem (1.5), in general, is nonlinear least squares. In this section, we shall present a decom-

position formula. Let $\boldsymbol{\phi}_i \in \mathbb{R}^{JK}$, $i = 1, 2, ...3I$, be defined by

$$
\begin{array}{ll}
& (\boldsymbol{\phi}_i) = (a_{i,1,1}e^{-\lambda_i t_1}, a_{i,2,1}e^{-\lambda_i t_1}, ..., a_{i,J,1}e^{-\lambda_i t_1}, ..., a_{i,J,K}e^{-\lambda_i t_K})^T \\
(2.1) \qquad & (\boldsymbol{\phi}_{I+i}) = (a_{i,1,1}e^{-\eta_i t_1}, a_{i,2,1}e^{-\eta_i t_1}, ..., a_{i,J,1}e^{-\eta_i t_1}, ..., a_{i,J,K}e^{-\eta_i t_K})^T \\
& (\boldsymbol{\phi}_{2I+i}) = (a_{i,1,1}, a_{i,2,1}, ..., a_{i,J,1}, ..., a_{i,J,K})^T, \quad i = 1, 2, ..., I.
\end{array}
$$

By (1.6) and (2.1), (1.5) can be reformulated into

$$
\min_{\boldsymbol{b},\boldsymbol{\beta}} r(\boldsymbol{b}, \boldsymbol{\beta}) \equiv \|\boldsymbol{d} - \boldsymbol{\Phi}(\boldsymbol{\beta})\boldsymbol{b}\|_2^2 \tag{2.2}
$$

where $\boldsymbol{d}$ is a JK-dimensional vector which consists of d_{jk} and $\boldsymbol{\Phi}$ a $JK \times 3I$ matrix defined by

$$
\boldsymbol{\Phi} = (\boldsymbol{\phi}_1, \boldsymbol{\phi}_2, ..., \boldsymbol{\phi}_{3I}). \tag{2.3}
$$

Let

$$
\begin{array}{l}
\boldsymbol{A}_k = (a_{ijk}) \in \mathbb{R}^{J \times I}, \\
\boldsymbol{\Lambda}_k = diag(e^{-\lambda_1 t_k}, e^{-\lambda_2 t_k}, ..., e^{-\lambda_I t_k}) \\
\boldsymbol{\Theta}_k = diag(e^{-\eta_1 t_k}, e^{-\eta_2 t_k}, ..., e^{-\eta_I t_k}).
\end{array} \tag{2.4}
$$

¿From (2.1) and (2.4), we have

$$
\begin{array}{l}
(\boldsymbol{\phi}_1, \boldsymbol{\phi}_2, ..., \boldsymbol{\phi}_I) = \begin{pmatrix} \boldsymbol{A}_1\boldsymbol{\Lambda}_1 \\ \boldsymbol{A}_2\boldsymbol{\Lambda}_2 \\ \vdots \\ \boldsymbol{A}_K\boldsymbol{\Lambda}_K \end{pmatrix} \\
(\boldsymbol{\phi}_{I+1}, \boldsymbol{\phi}_{I+2}, ..., \boldsymbol{\phi}_{2I}) = \begin{pmatrix} \boldsymbol{A}_1\boldsymbol{\Theta}_1 \\ \boldsymbol{A}_2\boldsymbol{\Theta}_2 \\ \vdots \\ \boldsymbol{A}_K\boldsymbol{\Theta}_K \end{pmatrix} \\
(\boldsymbol{\phi}_{2I+1}, \boldsymbol{\phi}_{2I+2}, ..., \boldsymbol{\phi}_{3I}) = \begin{pmatrix} \boldsymbol{A}_1 \\ \boldsymbol{A}_2 \\ \vdots \\ \boldsymbol{A}_K \end{pmatrix}.
\end{array} \tag{2.5}
$$

Moreover, let

$$
\begin{array}{c}
\boldsymbol{A} = diag(\boldsymbol{A}_1, \boldsymbol{A}_2, ..., \boldsymbol{A}_K) \\
\boldsymbol{\Lambda} = \begin{pmatrix} \Lambda_1 \\ \Lambda_2 \\ \vdots \\ \Lambda_K \end{pmatrix} \quad \boldsymbol{\Theta} = \begin{pmatrix} \Theta_1 \\ \Theta_2 \\ \vdots \\ \Theta_K \end{pmatrix} \quad \boldsymbol{\Upsilon} = \begin{pmatrix} E \\ E \\ \vdots \\ E \end{pmatrix}
\end{array} \tag{2.6}
$$

where E is the $I \times I$ identity matrix. Then, we have the following matrix decomposition

$$
\boldsymbol{\Phi} = (\boldsymbol{\phi}_1, \boldsymbol{\phi}_2, ..., \boldsymbol{\phi}_{3I}) = \boldsymbol{A}\boldsymbol{B}(\boldsymbol{\beta}) \tag{2.7}
$$

where

$$
\boldsymbol{B}(\boldsymbol{\beta}) = (\boldsymbol{\Lambda}, \boldsymbol{\Theta}, \boldsymbol{\Upsilon}). \tag{2.8}
$$

In (2.7), $\boldsymbol{A} \in \mathbb{R}^{JK \times IK}$ is a constant matrix independent of $\boldsymbol{\beta}$ and $\boldsymbol{B}(\boldsymbol{\beta}) \in \mathbb{R}^{IK \times 3I}$ is a sparse matrix function. A simplified model was applied by [7] for the study of myocardial viability using labeled fatty acids where

$$\xi_i(t) = A_i e^{-\lambda_i t}. \tag{2.9}$$

Let $\boldsymbol{\Phi}_s$, $\boldsymbol{A}_s$ and $\boldsymbol{B}_s$ denote the corresponding matrices for this simplified model. In this case,

$$\boldsymbol{B}_s(\boldsymbol{\beta}) = \boldsymbol{\Lambda_s}, \quad \boldsymbol{\Phi}_s = \boldsymbol{A}_s \boldsymbol{B}_s. \tag{2.10}$$

The matrix decomposition (2.7) is of significant importance for the following stability analysis.

3. Stability analysis. It has been noted that the functional $r(\boldsymbol{b}, \boldsymbol{\beta})$ has special structure: the linear parameter $\boldsymbol{b}$ and the nonlinear parameter $\boldsymbol{\beta}$. A numerical algorithm for such a least square problem was given in [4]. The approach therein involves the calculation of pseudo-inverse of $\boldsymbol{\Phi}$. For a given $\boldsymbol{\beta}$, the solution of the corresponding linear least squares problem can be given in terms of its pseudo-inverse. When C is rank deficient, its pseudo-inverse may be very sensitive. An example is as follows

$$C(\epsilon) = \begin{pmatrix} 1 & 0 \\ 0 & \epsilon \\ 0 & 0 \end{pmatrix},$$

which implies

$$\|C^+(\epsilon) - C^+(0)\| = 1/\epsilon.$$

Numerical algorithms for such rank deficient least squares problems are much less efficient.

3.1. Rank of $\boldsymbol{\Phi}(\boldsymbol{\beta})$. The above example shows that a rank deficient model is itself unstable. The corresponding problem for this SPECT model is to consider the rank of matrix $\boldsymbol{\Phi} = \boldsymbol{AB}$. By (2.6) and (2.8), $\boldsymbol{B}$ is similar to a block diagonal matrix $\boldsymbol{B} = diag(\boldsymbol{B}_1, \boldsymbol{B}_2, ..., \boldsymbol{B}_I)$ where $\boldsymbol{B}_i \in \mathbb{R}^{K \times 3}$ and therefore,

$$Rank \boldsymbol{B} = \sum_{i=1}^{I} Rank \boldsymbol{B}_i. \tag{3.1}$$

The following Lemma can be obtained by noting the Vandermonde matrix structure of each $\boldsymbol{B}_i$.

Lemma 3.1 *Let $\boldsymbol{B}(\boldsymbol{\beta})$ be defined in (2.8). Then*

$$Rank\, \boldsymbol{B}(\boldsymbol{\beta}) = \sum_{i=1}^{I} c_i \tag{3.2}$$

where c_i denotes the number of distinct elements in the set $\{\lambda_i, \eta_i, 0\}$, $i = 1, 2, ..., I$.

Notice from Lemma 3.1 that $\boldsymbol{B}(\boldsymbol{\beta})$ is full rank when λ_i, η_i and 0 are distinct for each i.

Let $\Pi_{J,K} = \{s_j, t_k\}$ define a partition on $\Omega = [0, \sqrt{2}] \times [0, T]$. We assume that

(i) $\{s_j\}$ is a uniform partition on $[0, \sqrt{2}]$ ($\Delta s = s_{j+1} - s_j = \frac{\sqrt{2}}{J}$) and

$$\tau_1 \Delta s = s_1 < s_2 < ... < s_J = \sqrt{2} - \tau_1 \Delta s.$$

where $0 \leq \tau_1 \leq 1$;

(ii) $\{t_k\}$ is a uniform partition on $[0, T]$ ($\Delta t = t_{k+1} - t_k = \frac{T}{K}$) and

$$\tau_2 \Delta t = t_1 < t_2 < ... < t_K = T - \tau_2 \Delta t$$

where $0 \leq \tau_2 \leq 1$. In general, we take $\tau_1 = \tau_2 = 1/2$. The typical geometry and its partition are shown in Figure 2 which is useful in the proof of our main theorem.

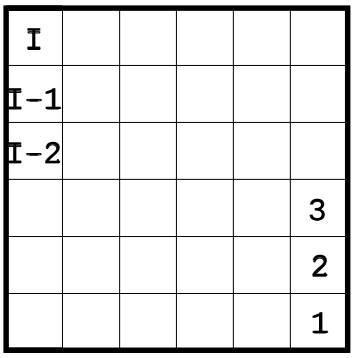

FIG. 2. *A typical geometry of image*

Lemma 3.2 *Let* $(\boldsymbol{\Phi}, \boldsymbol{d})$ *denote a SPECT model on the partition* $\Pi_{J,K}$ *with the assumptions (i)-(ii) and* $\{\boldsymbol{A}_k\}$ *be defined in (2.4). Then there exist positive integer numbers* $\bar{K}$ *and* $\bar{J}$ *such that when* $K > \bar{K}$ *and* $J > \bar{J}$, *at least three of* $\{\boldsymbol{A}_1, \boldsymbol{A}_2, ..., \boldsymbol{A}_K\}$ *are full rank.*

Proof By (1.4) and (2.4), $(\boldsymbol{A}_k)_{ji} = a_{ijk}$ represents the length of the intersection of the jth ray coming from the angle of the kth projection within the ith pixel.

We denote by t_k the angle of the kth projection. Then there exists $\bar{K} > 0$ such that when $K \geq \bar{K}$, there are three of $\{t_k\}_{k=1}^{K}$ in the interval $[arctan(I_1), \frac{\pi}{2})$. Without loss of generality, we assume that

$$arctan(I_1) \leq t_{k_1} < t_{k_1+1} < t_{k_1+2} < \frac{\pi}{2}. \tag{3.3}$$

For each t_l, $l = k_1, k_1 + 1, k_1 + 2$, we denote by $\{L_1, L_2, ..., L_J\}$ the corresponding rays. When J is large enough, there exists a subset, denoted by $\{L_{j_1}, L_{j_2}, ..., L_{j_I}\}$, which satisfies:

L_{j_1} only passes through pixel 1 (*i.e.*, $a_{1j_1 l} \neq 0$ and $a_{pj_1 l} = 0$ for $p > 1$);

L_{j_2} only passes through pixel 2 and possibly, pixel 1 (*i.e.*, $a_{2j_2 l} \neq 0$ and $a_{pj_2 l} = 0$ for $p > 2$);

For any i, L_{j_i} only passes through pixel i and possibly, those pixels passed by L_{j_p}, $p < i$ (*i.e.*, $a_{ij_i l} \neq 0$ and $a_{pj_i l} = 0$ for $p > i$, see Figure 3).

The submatrix corresponding to the rows j_1, j_2, ..., j_I of $\boldsymbol{A}_l$ is $I \times I$ nonsingular triangular. Then $\boldsymbol{A}_l$, $l = k_1, k_1 + 1, k_1 + 2$, is full rank. ∎

Our main result is given in the following theorem.

Theorem 3.1 *Let* $(\mathbf{\Phi}, \boldsymbol{d})$ *denote a SPECT model on the partition* $\Pi_{J,K}$ *with* I *pixels and satisfying assumptions (i)-(ii). Then there exist positive integer numbers* $\bar{K}$ *and* $\bar{J}$ *such that when* $K > \bar{K}$ *and* $J > \bar{J}$,

$$Rank\mathbf{\Phi}(\beta) = \sum_{i=1}^{I} c_i \equiv c. \tag{3.4}$$

Proof . By Lemma 3.2, we can assume that $\boldsymbol{A}_{k_1}$, $\boldsymbol{A}_{k_2}$ and $\boldsymbol{A}_{k_3}$ are full rank. Then the submatrix corresponding to the k_1th, k_2th and $k_3 th$ block rows of $\mathbf{\Phi}$ is

$$\begin{pmatrix} \boldsymbol{A}_{k_1} & 0 & 0 & 0 & \cdots & 0 \\ 0 & \boldsymbol{A}_{k_2}, & 0 & 0 & \cdots & 0 \\ 0 & 0 & \boldsymbol{A}_{k_3} & 0 & \cdots & 0 \end{pmatrix} \boldsymbol{B} = \begin{pmatrix} \boldsymbol{A}_{k_1} & 0 & 0 \\ 0 & \boldsymbol{A}_{k_2} & 0 \\ 0 & 0 & \boldsymbol{A}_{k_3} \end{pmatrix} \begin{pmatrix} \mathbf{\Lambda}_{k_1} & \mathbf{\Theta}_{k_1} & \boldsymbol{E} \\ \mathbf{\Lambda}_{k_2} & \mathbf{\Theta}_{k_2} & \boldsymbol{E} \\ \mathbf{\Lambda}_{k_3} & \mathbf{\Theta}_{k_3} & \boldsymbol{E} \end{pmatrix}. \tag{3.5}$$

By Lemma 3.1,

$$Rank\mathbf{\Phi} = Rank \begin{pmatrix} \mathbf{\Lambda}_{k_1} & \mathbf{\Theta}_{k_1} & \boldsymbol{E} \\ \mathbf{\Lambda}_{k_2} & \mathbf{\Theta}_{k_2} & \boldsymbol{E} \\ \mathbf{\Lambda}_{k_3} & \mathbf{\Theta}_{k_3} & \boldsymbol{E} \end{pmatrix} = c. \quad \blacksquare \tag{3.6}$$

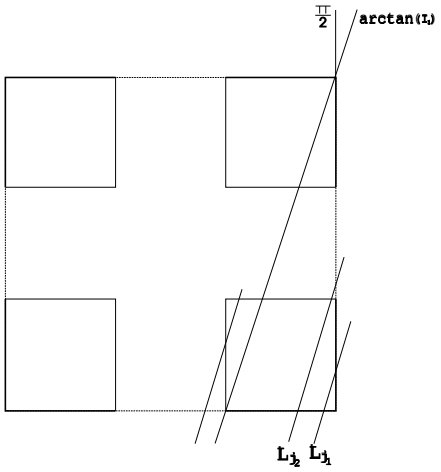

FIG. 3. *The rays* L_{j1}, L_{j2},..., L_{jI} *corresponding to* l*th projection*

Corollary 3.1 *If* $(\lambda_i, \eta_i, 0)$ *are distinct for each* $i = 1, 2, ..., I$, *there exist* $\bar{K} > 0$ *and* $\bar{J} > 0$ *such that when* $K > \bar{K}$ *and* $J > \bar{J}$, $\mathbf{\Phi}$ *is full rank.*

For this underlying SPECT model, the physical parameters λ and η always satisfy $\lambda_i > \eta_i > 0$ for each i. Then $\mathbf{\Phi}$ is full rank if the data collected are large enough.

Remarks

TABLE 1
Rank of $\mathbf{\Phi}$

I	K	J(even)	*Rank* of $\mathbf{\Phi}$
2×2	2	all	rank deficient
	4	all	rank deficient
	6	2	rank deficient
		4	full rank
4×4	4	all	rank deficient
	6	12	rank deficient
		20	full rank
	8	10	rank deficient
		12	full rank
8×8	12	20	rank deficient
		24	full rank
16×16	24	24	rank deficient
	28	32	full rank

Notice from the proof of Lemma 3.2 and Theorem 3.1 that we can obtain an estimate for $\bar{J}$ and $\bar{K}$ as follows. First, since Δs is the distance between two sequent rays, by a straightforward calculation (3.3) requires

$$0 < 3\Delta t \leq \frac{\pi}{2} - arctan(I_1) \quad \text{and} \quad 0 < \Delta s \leq \frac{cos(t_3)}{I_1} \tag{3.7}$$

which implies

$$\begin{aligned} \bar{J} &= [\tfrac{I_1}{cos(t_3)}] + 1 \\ \bar{K} &= [\tfrac{3T}{\frac{\pi}{2} - arctan(I_1)}] + 1 \end{aligned} \tag{3.8}$$

where [.] denote the integer part. The above estimates are available for any $0 \leq \tau_2 \leq 1$ and $T > 0$. Most usually, $T = \pi$ and $\tau_2 = 0$ or $\tau_2 = \Delta s/2$. In this case, one can replace 3 with 2.5 in (3.7) and (3.8) since $t_{k_1+2} = \frac{\pi}{2}$ when K is odd and $t_{k_1+2} = \frac{\pi}{2} - \frac{\Delta t}{2}$ when K is even. ¿From (3.7)-(3.8), when I is large, we have

$$\bar{K} \approx \sqrt{3I} \quad \text{and} \quad \bar{J} \approx I. \tag{3.9}$$

(3.9) gives an estimate of $\bar{J}$ and $\bar{K}$. The optimal estimate is unknown. It is obvious from Corollary 3.1 that the simplified model is full rank if K and J are large enough. The corresponding estimates for this simplified model can be obtained by simply replacing 3 with 1 in (3.7)-(3.9).

Next, we present some numerical results for the model (1.5) in Table 1 in which we assume that $c_i = 3$ for all i. The numerical results corresponding to the simplified model (2.9) are given in Table 2. ¿From the numerical tests, a conjecture for the optimal estimate could be

$$\bar{J} = O(\sqrt{I}) \quad \text{and} \quad \bar{K} = O(\sqrt{I}).$$

Although we have restricted the discussion on the SPECT model (1.5) with the assumptions (i)-(ii), it is obvious that Theorem 3.1 can be extended to arbitrary convex domains and non-uniform meshes. The three-dimensional SPECT model can be similarly analysed. Generalization for non-rectangular pixels are not obvious but less important.

TABLE 2
Rank of $\mathbf{\Phi}_s$

I	K	J(even)	*Rank* of $\mathbf{\Phi}$
2×2	2	all	rank deficient
	4	2	full rank
4×4	4	all	rank deficient
	6	4	rank deficient
		6	full rank
	8	2	rank deficient
		4	full rank
8×8	8	all	rank deficient
	10	12	rank deficient
		14	full rank
16×16	18	20	rank deficient
	22	26	full rank

3.2 The stability of full rank models. Let $\|.\|_\infty$ define a norm as follows:

$$\|u\|_\infty = max_l|u_l|, \quad u \in \boldsymbol{R}^m$$

and consider the corresponding matrix norm. For a full rank linear least squares problem, stability depends upon the **condition number** of $\mathbf{\Phi}$ which is defined by

$$\mathcal{K}(\mathbf{\Phi}) \equiv \|\mathbf{\Phi}\|_2 \cdot \|(\mathbf{\Phi}^T\mathbf{\Phi})^{-1}\|_2 \cdot \|\mathbf{\Phi}^T\|_2. \tag{3.10}$$

The estimates of $\|\mathbf{\Phi}\|_2$ and $\|\mathbf{\Phi}^T\|_2$ are given in the following lemma.

Lemma 3.3 *For any* $\boldsymbol{\beta} \geq 0$,

$$\|\mathbf{\Phi}\|_2 \leq \sqrt{\frac{6JK}{I}} \quad \textit{and} \quad \|\mathbf{\Phi}^T\|_2 \leq \sqrt{\frac{6JK}{I}}. \tag{3.11}$$

Moreover,

$$\|\mathbf{\Phi}_s\|_2 \leq \sqrt{\frac{2JK}{I}} \quad \textit{and} \quad \|\mathbf{\Phi}_s^T\|_2 \leq \sqrt{\frac{2JK}{I}}. \tag{3.12}$$

Proof By the matrix decomposition (2.7), we have

$$\|\mathbf{\Phi}\|_2^2 = \rho(\boldsymbol{B}^T\boldsymbol{A}^T\boldsymbol{A}\boldsymbol{B}) \leq \|\boldsymbol{B}^T\|_\infty \cdot \|\boldsymbol{A}^T\boldsymbol{A}\|_\infty \cdot \|\boldsymbol{B}\|_\infty \tag{3.13}$$

where $\rho(C)$ denotes the spectral radius of matrix C. It follows from (2.4), (2.6) and (2.8) that

$$\|\boldsymbol{B}\|_\infty = 3, \quad \|\boldsymbol{B}^T\|_\infty = K \tag{3.14}$$

and

$$\boldsymbol{A}^T\boldsymbol{A} = diag(\boldsymbol{A}_1^T\boldsymbol{A}_1, \boldsymbol{A}_2^T\boldsymbol{A}_2, \cdots, \boldsymbol{A}_K^T\boldsymbol{A}_K). \tag{3.15}$$

Since $(\boldsymbol{A}_k)_{ji} = a_{ijk}$ and $\sum_{i=1}^{I} a_{ijk}$ represent the length of the intersection of the jth ray coming from the angle of the kth projection within the ith pixel and this image region Ω, respectively, we have

$$0 \leq a_{ijk} \leq \frac{\sqrt{2}}{I_1} \quad \text{and} \quad \sum_{i=1}^{I} a_{ijk} \leq \sqrt{2}. \tag{3.16}$$

For any given k and i, there are at most $[\frac{J}{I_1}]$ rays which pass through the ith pixel and

$$\sum_{j=1}^{J} a_{ijk} \leq [\frac{J}{I_1}]\frac{\sqrt{2}}{I_1} \leq \frac{\sqrt{2}J}{I}. \tag{3.17}$$

Then

$$\|\boldsymbol{A}_k^T \boldsymbol{A}_k\|_\infty \leq \|\boldsymbol{A}_k^T\|_\infty \cdot \|\boldsymbol{A}_k\|_\infty \leq \frac{2J}{I} \tag{3.18}$$

and therefore, it follows from (3.15)-(3.20) that

$$\|\boldsymbol{\Phi}\|_2 \leq \sqrt{3K \max_k \|\boldsymbol{A}_k^T \boldsymbol{A}_k\|_\infty} \leq \sqrt{\frac{6KJ}{I}}. \tag{3.19}$$

Now, (3.14) can be obtained similarly. ∎

It will be useful to recall that for a symmetric matrix S and any principal submatrix S_p, we have the following inequality

$$\sigma(S) \leq \sigma(S_p) \leq \rho(S_p) \leq \rho(S) \tag{3.20}$$

where $\sigma(S)$ denotes the minimal eigenvalue of matrix S.

Theorem 3.2 *Let* $(\boldsymbol{\Phi}, \boldsymbol{d})$ *and* $(\bar{\boldsymbol{\Phi}}, \bar{\boldsymbol{d}})$ *define two SPECT models on the partitions* $\Pi_{J,K} = \{\theta_j, t_k\}$ *and* $\Pi_{\bar{J},\bar{K}} = \{\bar{\theta}_j, \bar{t}_k\}$, *respectively and* $\Pi_{J,K} \subset \Pi_{\bar{J},\bar{K}}$. *Then*

$$\begin{aligned} \|\boldsymbol{\Phi}\|_2 &\leq \|\bar{\boldsymbol{\Phi}}\|_2 \\ \|\boldsymbol{\Phi}^T\|_2 &\leq \|\bar{\boldsymbol{\Phi}}^T\|_2 \\ \|(\boldsymbol{\Phi}^T\boldsymbol{\Phi})^{-1}\|_2 &\geq \|(\bar{\boldsymbol{\Phi}}\bar{\boldsymbol{\Phi}}^T)^{-1}\|_2. \end{aligned} \tag{3.21}$$

Proof Since $\Pi_{J,K} \subset \Pi_{\bar{J},\bar{K}}$, $\boldsymbol{\Phi}$ is a submatrix of $\bar{\boldsymbol{\Phi}}$ and therefore, $\boldsymbol{\Phi}\boldsymbol{\Phi}^T$ is a principal submatrix of $\bar{\boldsymbol{\Phi}}\bar{\boldsymbol{\Phi}}^T$ and $\bar{\boldsymbol{\Phi}}^T\bar{\boldsymbol{\Phi}} = \boldsymbol{\Phi}^T\boldsymbol{\Phi} + S$ where S is a symmetric and nonnegative definite matrix. Theorem 3.2 follows immediately by noting (3.22) and

$$\|(\bar{\boldsymbol{\Phi}}^T\bar{\boldsymbol{\Phi}})^{-1}\|_2 = \frac{1}{\sigma(\boldsymbol{\Phi}^T\boldsymbol{\Phi})}. \tag{3.22}$$ ∎

Notice from Theorem 3.2 that in some sense, $\|\boldsymbol{\Phi}\|_2$ and $\|\boldsymbol{\Phi}^T\|_2$ are monotone decreasing functions and $\|(\boldsymbol{\Phi}^T\boldsymbol{\Phi})^{-1}\|_2$ is a monotone increasing function. However, monotonicity is not apparent for the condition number $\mathcal{K}(\boldsymbol{\Phi})$.

Theorem 3.3 *Let* $(\boldsymbol{\Phi}, \boldsymbol{d})$, $(\boldsymbol{\Phi}_1, \boldsymbol{d}_1)$ *and* $(\boldsymbol{\Phi}_2, \boldsymbol{d}_2)$ *define three SPECT models on the partitions* $\Pi_{J,K}$, Π_{J_1,K_1} *and* Π_{J_2,K_2}, *respectively where* $(\Pi_{J_1,K_1} \bigcup \Pi_{J_2,K_2}) \subset \Pi_{J,K}$. *and* $(\Pi_{J_1,K_1} \bigcap \Pi_{J_2,K_2}) = 0$ *Then*

$$\|(\boldsymbol{\Phi}^T\boldsymbol{\Phi})^{-1}\|_2 \leq \frac{1}{2} max\{\|(\boldsymbol{\Phi}_1^T\boldsymbol{\Phi}_1)^{-1}\|_2, \|(\boldsymbol{\Phi}_2^T\boldsymbol{\Phi}_2)^{-1}\|_2\}. \tag{3.23}$$

Proof Since $(\Pi_{J_1,K_1} \bigcup \Pi_{J_2,K_2}) \subset \Pi_{J,K}$ and $(\Pi_{J_1,K_1} \bigcap \Pi_{J_2,K_2}) = 0$, $\begin{pmatrix} \mathbf{\Phi}_1 \\ \mathbf{\Phi}_2 \end{pmatrix}$ is a submatrix of $\mathbf{\Phi}$ and moreover, we have

$$\mathbf{\Phi}^T\mathbf{\Phi} = \begin{pmatrix} \mathbf{\Phi}_1 \\ \mathbf{\Phi}_2 \end{pmatrix}^T \begin{pmatrix} \mathbf{\Phi}_1 \\ \mathbf{\Phi}_2 \end{pmatrix} + S$$

where S is a symmetric and nonnegative definite matrix. Then

$$\sigma(\mathbf{\Phi}^T\mathbf{\Phi}) = \min_{\|x\|_2=1} x^T\mathbf{\Phi}^T\mathbf{\Phi}x \geq \min_{\|x\|_2=1} x^T\mathbf{\Phi}_1^T\mathbf{\Phi}_1x + \min_{\|x\|_2=1} x^T\mathbf{\Phi}_2^T\mathbf{\Phi}_2x \tag{3.24}$$

which leads to

$$\sigma(\mathbf{\Phi}^T\mathbf{\Phi}) \geq 2\min\{\sigma(\mathbf{\Phi}_1^T\mathbf{\Phi}_1), \sigma(\mathbf{\Phi}_2^T\mathbf{\Phi}_2)\}. \tag{3.25}$$

By (3.24), we have

$$\|(\mathbf{\Phi}^T\mathbf{\Phi})^{-1}\|_2 \leq \frac{1}{2}\frac{1}{min\{\sigma(\mathbf{\Phi}_1^T\mathbf{\Phi}_1), \sigma(\mathbf{\Phi}_2^T\mathbf{\Phi}_2)\}} \leq \frac{1}{2}max\{\|(\mathbf{\Phi}_1^T\mathbf{\Phi}_1)^{-1}\|_2, \|(\mathbf{\Phi}_2^T\mathbf{\Phi}_2)^{-1}\|_2\}. \quad \blacksquare \tag{3.26}$$

In the assumptions (i)-(ii), the partition is related to the two parameters τ_1 and τ_2 $(0 \leq \tau_1, \tau_2 \leq 1)$. We define

$$h(J, K, \tau_1, \tau_2) \equiv \|(\mathbf{\Phi}^T\mathbf{\Phi})^{-1}\|_2.$$

Theorem 3.4 *Let $(\mathbf{\Phi}, \boldsymbol{d})$ define a SPECT model on the partition $\Pi_{J,K}$ with $J = J_1 \cdot 2^m$ and $K = K_1 \cdot 2^n$ where J_1 and K_1 be positive integers such that the models on the partition Π_{J_1,K_1} are full rank. Then*

$$\mathcal{K}(\mathbf{\Phi}) \leq \bar{c} \tag{3.27}$$

where $\bar{c}$ is a constant independent of m and n.

Proof . Applying Theorem 3.3 repeatedly to problems of "half-size", we have

$$\|(\mathbf{\Phi}^T\mathbf{\Phi})^{-1}\|_2 \leq \frac{1}{2^m \cdot 2^n} \cdot \max_{\tau_1,\tau_2} h(J_1, K_1, \tau_1, \tau_2). \tag{3.28}$$

Then Theorem 3.4 follows immediately from Lemma 3.3 and the last equation, where

$$\bar{c} = \frac{6J_1K_1}{I} \cdot \max_{\tau_1,\tau_2} h(J_1, K_1, \tau_1, \tau_2). \quad \blacksquare \tag{3.29}$$

When J_1 and K_1 are large enough, $\max_{\tau_1,\tau_2} h(J_1, K_1, \tau_1, \tau_2)$ is approximately a constant. Then $\bar{c}$ only depends upon J_1 and K_1.

In Table 3, we present some numerical results to confirm our analysis. The following observations can be made from this table:

$$\begin{array}{l} \|\mathbf{\Phi}\|_2 = O(\sqrt{JK}) \\ \|\mathbf{\Phi}^T\|_2 = O(\sqrt{JK}) \\ \|(\mathbf{\Phi}^T\mathbf{\Phi})^{-1}\|_2 = O(\frac{1}{JK}) \\ \mathcal{K}(\mathbf{\Phi}) = O(1) \end{array} \tag{3.30}$$

when J and K are large enough. It is reassuring that the numerical results are in good agreement with our theoretical analysis.

TABLE 3
The condition number $\mathcal{K}(\mathbf{\Phi}_s)$ for $\lambda = 1.0$, $\eta = 0.1$

I	$J \times K$	$\|\|\mathbf{\Phi}\|\|_2$	$\|\|\mathbf{\Phi}^T\|\|_2$	$\|\|(\mathbf{\Phi}^T\mathbf{\Phi})^{-1}\|\|_2$	$\mathcal{K}(\mathbf{\Phi})$
8×8	10×10				rank deficient
	20×20	0.9061	0.8542	115.6	89.46
	40×20	1.279	1.255	43.23	69.39
	20×40	1.233	1.203	54.52	80.87
	40×40	1.741	1.739	20.91	63.32
	80×40	2.415	2.452	10.18	60.28
	40×80	2.457	2.411	10.44	61.82
16×16	20×20				rank deficient
	40×40	2.827	2.754	7.246D7	5.619D8
	80×40	3.981	3.903	3.459D6	5.374D7
	40×80	3.882	3.829	3.822D6	5.681D7
	80×80	5.622	5.599	1.105D6	3.478D7
	120×80	6.882	6.849	6.698D6	3.154D7
	80×120	6.899	6.853	6.729D6	3.181D7

4. Numerical Experiments. In this section, we report on some experimentation to show the stability of the SPECT models. We consider only a linear model in which

$$\xi_i(t) = A_i e^{-\lambda t} + B_i e^{-\eta t} + C_i, \quad i = 1, 2, ..., I \tag{4.1}$$

where λ and η are predetermined constants. The analytic solution is given by

$$\begin{aligned} &A = B = C = 2 \quad 6/8 \le x \le 7/8,\ 2/8 \le y \le 3/8 \\ &A = B = C = 3 \quad 2/8 \le x \le 3/8,\ 6/8 \le y \le 7/8 \\ &A_i = B_i = C_i = 0 \quad \text{other}. \end{aligned} \tag{4.2}$$

We use both 8×8 ($I = 64$) and 16×16 ($I = 256$) images in our test. The exact value of $\boldsymbol{d}$ is obtained from the analytic solution. Due to physical measurement error, the data $\boldsymbol{d}$ is often collected in the detector with a statistical noise,

$$\boldsymbol{d}_\epsilon = \boldsymbol{d} + \delta \tag{4.3}$$

where δ can be considered as a normal distribution. In this numerical study, we assume that the variance of this distribution is 10^{-4} (or 10000 counts). We denote by $\{\xi_i^\delta(t)\}$ perturbated solution. The perturbation error is defined by

$$\epsilon_i = max_k |\xi_i(t_k) - \xi_i^\delta(t_k)| \tag{4.4}$$

The numerical results are given in Figures 4-5 with different $J \times K$. It is obvious that the perturbation error is related to the physical parameters λ_i and η_i and significantly decreases as J and/or K increase. The simplified model is much more stable than the corresponding full model. We also tested the SPECT model for different numbers of pixels and counts. For a model with 1000 counts, we will obtain the similar results when larger J and K are used. The error usually increases as the number of pixels increases. Throughout, the numerical experiments were performed on a Sun SPARC+1 in double precision, using standard IMSL routines for solving the least squares and eigenvalue problems.

5. Conclusions. A stability analysis for a class of dynamic SPECT models arising from the medical imaging studies has been presented. This gives a clear indication

how one can produce a stable model. Small J and K often give a rank deficient model. The condition number is decreasing and is eventually bounded by a constant as J and K increase. However, in practice, J and K are also restricted by the equipment used.

While only limited experiments have been performed, the results are quite encouraging. It is our intention to perform a more general theoretical analysis of the stability problems. More extensive numerical tests for general nonlinear SPECT models and corresponding efficient numerical algorithms are under investigation.

Acknowledgements. The authors thank Drs Scott Barney, Anna Celler and Robert D. Russell for their helpful suggestions and comments.

REFERENCES

[1] A.S. Abdulmassih, S. Iskandrian and H.R. Schelbert, *Myocardial viability assessment,* J. Nucl. Med., 35(1994), 1S–58S.

[2] R.N Bracewell and A.C. Riddle, *Inversion of fan beams in radio astronomy,* Astron. J., 150(1967), pp.427-434.

[3] T.F. Budinger, G.T. Gullberg, *Three dimensional reconstruction in nuclear medicine by iterative least squares and Fourier transform techniques,* IEEE on Trans. Nuclear Science, 21(1974), pp. 2-20.

[4] I. Guttman, V. Pereyra and H.D. Scolnik, *Least squares estimation for a class of nonlinear models,* Centre de Recherche Mathematique, University of Montreal, 1971.

[5] M.P.J Hudon, D.M. Lyster, W.R.E Jamieson, A.K. Qayumi, C. Sartori and H.A. Dougan, *The metabolism of (^{123}I)-iodophenyl pentadecanoic acid in a surgically induced canine model of regional ischemia,* Eur. J. Nucl. Med., 16(1990), pp.199–204.

[6] G.D. Hutchins, W.L. Rogers, P. Chiao, R.R. Raylman and B.W. Murphy, *Constrained least squares filtering in high resolution PET and SPECT imaging,* IEEE on Trans. Nuclear Science, 37(1990), pp. 647–651.

[7] M.A. Limber, M.N. Limber, A. Celler, J.S. Barney and J.M. Borwein, , *Direct reconstruction of functional parameters for dynamic SPECT* , submitted.

[8] J. Radon, *Uber die bestimmung von funktionen durch ihre integralwerte langs gewisser mannigfaltigkelten,* Ber. Verh. K. Saechs. Ges. Wiss, Math-Phys. K1, 69(1917), pp.262-279.

[9] A. Papoulis, *Systems and Transforms with Applications to Optics*, McGraw-Hill, New York, 1969.

[10] M.J. van Eenige, F.C. Visser, C.M.B. Duwel, P.D. Bezemer, G. Westera, A.J.P. Karreman and J.P. Roos, *Analysis of myocardial time-activity curves of ^{123}I- heptadecanoic acid I, Curve Fitting,* Nucl-Med., 26(1987), pp.241–247.

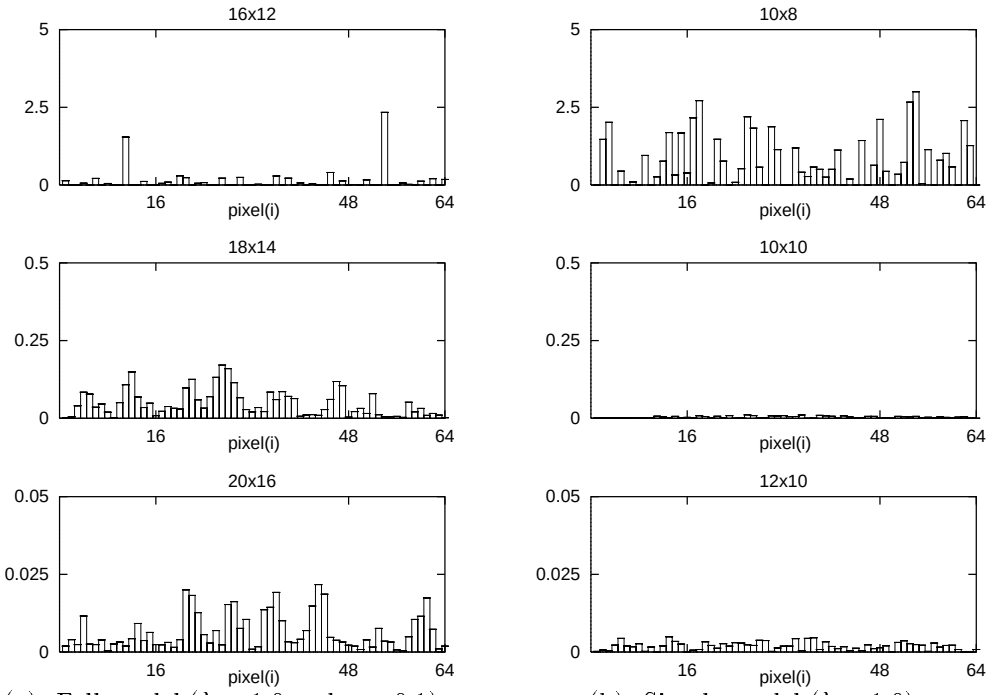

(a). Full model ($\lambda = 1.0$ and $\eta = 0.1$). (b). Simple model ($\lambda = 1.0$).

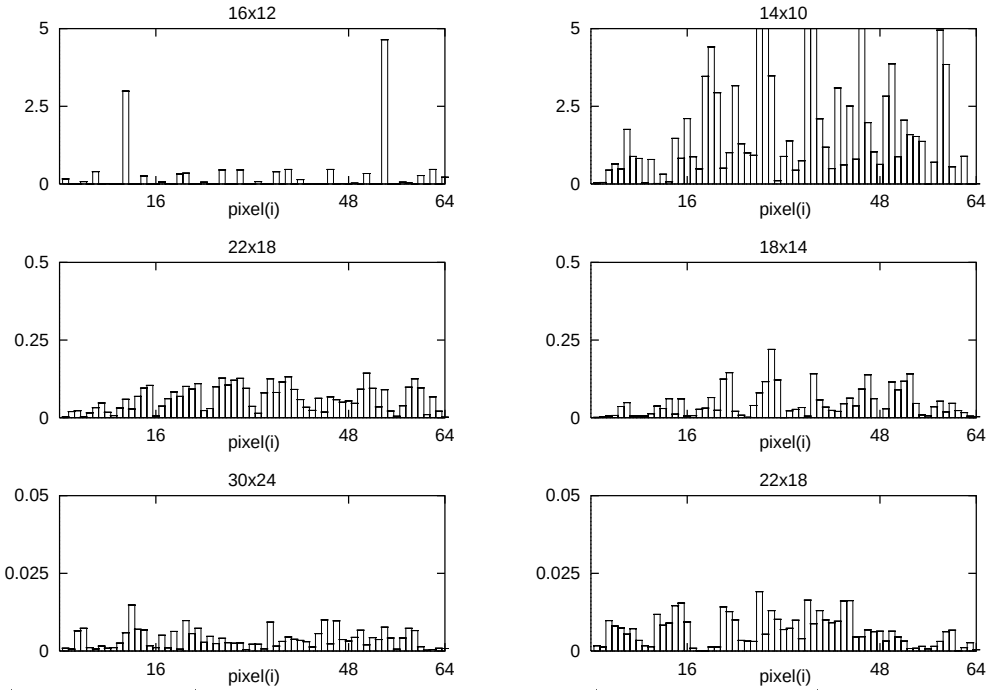

(c). Full model ($\lambda = 5.0$ and $\eta = 1.0$). (d). Simple model ($\lambda = 5.0$).

FIG. 4. *The error ϵ_i of the linear model with 8×8 pixels and noise.*

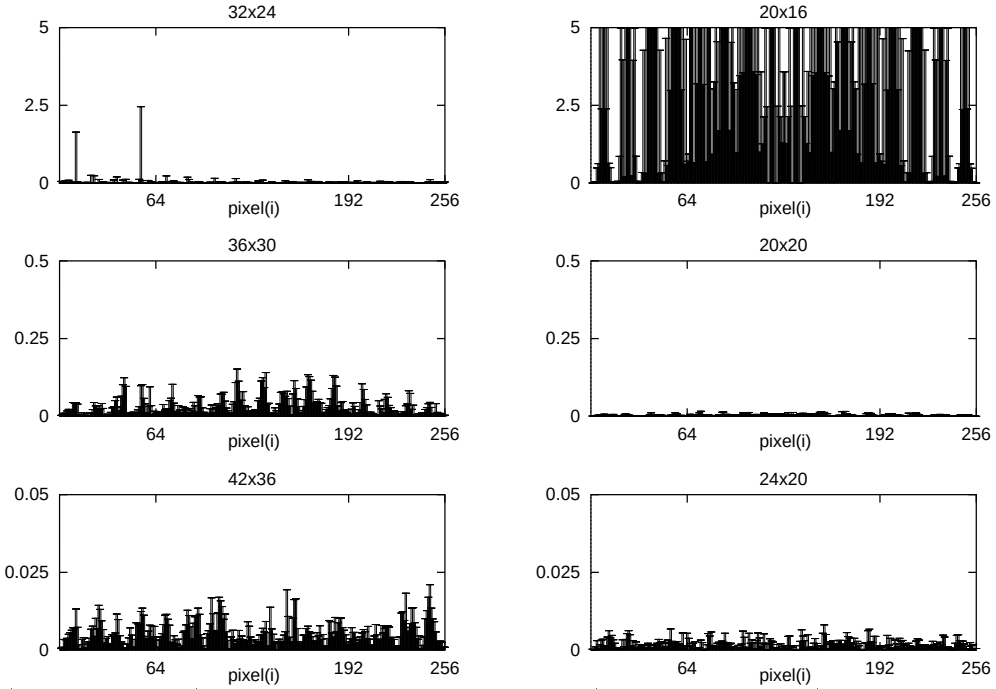

(a). Full model ($\lambda = 1.0$ and $\eta = 0.1$).

(b). Simple model ($\lambda = 1.0$).

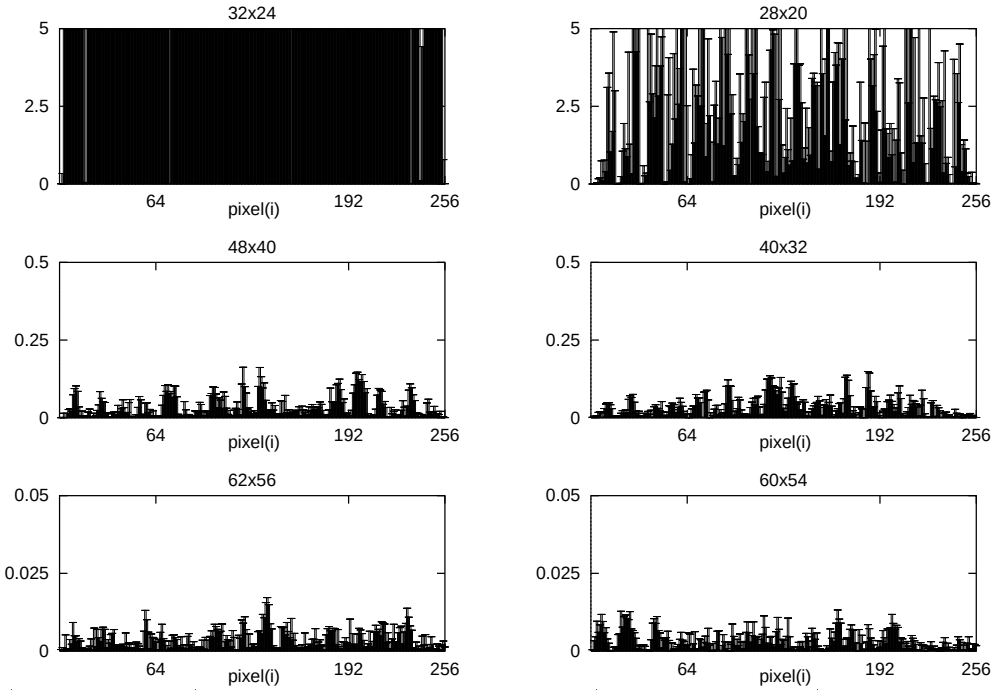

(c). Full model ($\lambda = 5.0$ and $\eta = 1.0$).

(d). Simple model ($\lambda = 5.0$).

FIG. 5. *The error of the linear model with* 16×16 *pixels and noise.*